Density and index of refraction of water ice films vapor deposited at low temperatures

M. S. Westley, G. A. Baratta, and R. A. Baragiola

Citation: **108**, 3321 (1998); doi: 10.1063/1.475730
View online: http://dx.doi.org/10.1063/1.475730
View Table of Contents: http://aip.scitation.org/toc/jcp/108/8
Published by the American Institute of Physics

Density and index of refraction of water ice films vapor deposited at low temperatures

M. S. Westley[a] G. A. Baratta[b] and R. A. Baragiola[c]
Laboratory for Atomic and Surface Physics, Engineering Physics, University of Virginia, Charlottesville, Virginia 22901

(Received 10 October 1997; accepted 19 November 1997)

The density of 0.5–3 μm thick vapor-deposited films of water ice were measured by combined optical interferometry and microbalance techniques during deposition on an optically flat gold substrate from a capillary array gas source. The films were of high optical quality with an index of refraction of 1.29 ± 0.01 at 435.8 nm, a density of 0.82 ± 0.01 g/cm^3, and a porosity of 0.13 ± 0.01. In contrast to previous studies, none of the measured properties exhibited any significant variation with growth rate or temperature over the range studied (0.6–2 nm/min, 20–140 K). © *1998 American Institute of Physics.* [S0021-9606(98)50408-4]

I. INTRODUCTION

Although the properties of water ice have been studied extensively near fusion temperatures at atmospheric pressure,[1,2] large gaps still exist in our knowledge of its properties at the low temperatures and pressures found in space environments[3] and cryogenic laboratory systems.[4] Water ice grown by vapor deposition at low temperatures ($<$150 K) is an important substance in many planetary environments such as the surfaces of satellites of the outer planets, the polar caps of Mars, the surfaces of comets, interstellar grains, and planetary rings. Properties of water ice that are of special interest in planetary environments include sublimation rates, thermal conductivity, density, microstructure, gas absorbance, and the effects of photon and particle irradiation.

A fundamental problem facing studies of vapor deposited water ice is that many of its properties are not reproducible among different laboratories. An example is the variation of sublimation and crystallization rates of the amorphous phase below 140 K. These properties were recently shown to depend on the amorphous to crystalline content of the ice deposits,[5] which depend on growth temperature and on the type of substrate[6,7] for reasons that are not fully understood. Widely varying values also exist for properties important for the evolution of icy surfaces in space, like thermal conductivity,[8,9] condensation coefficient,[10–15] and effective surface area for gas absorption.[16–23] In this work, we focus on the density of vapor deposited ice and its dependence on growth conditions. Ice films with very different values of average density and with porosities[24,25] ranging from 0.05 to $\sim$0.6 have been reported. From the large effective areas for absorption of gases at low temperatures, it can be inferred that the porosity is due to interconnected micropores,[19] of unknown morphology.

There have been conflicting reports of the index of refraction[11,14,15,26–28] which correspond to different values of density and porosity, quantities related by the Lorentz–Lorenz relation.[29] The uniformity of the ice deposits is also important. Several optical interference experiments have shown numerous, weakly attenuated, interference cycles vs film thickness, indicating smooth and uniform films.[15,30] However, some experiments have produced ice films with appear to the eye to have an extremely rough, needlelike structure.[21,31] Another experimental variable which may affect morphology, to be discussed later in the paper, is the direction of incidence of the molecules onto the surface.

Some of the different properties of water ice can be attributed to different microscopic structure. Ice condensed from the vapor phase at below 100–130 K, depending on growth rate, is amorphous, with varying content of crystal grains.[5] Amorphous ice is not a clearly defined structure, and different polymorphs have been found,[32–34] that can be identified by their density ρ. The common low density form results for growth temperatures between 30 and 135 K; its intrinsic density (not including micropores), is $\rho = 0.94$ g/cm^3, as measured by flotation[35] and by x-ray diffraction.[36] A lower effective density results if the void pore space is included in the calculation. Seiber *et al.*[37] measured a density of 0.81 ± 0.01 g/cm^3 at 82 K using mass and optical interference measurements, such as the one described here, which average over the sample. This implies a porosity of 0.14. Recent optical studies[11–15] found densities that decrease with deposition temperature, from a plateau value of 0.93 g/cm^3 at 120–150 K to as low as $\sim$0.6 g/cm^3 at 20 K (Ref. 15). Such low values at 20 K are consistent with those from other studies[20,25] but contrast with a recent report that ice grown at 5 K has no discernible porosity.[38] Below about 40 K, condensation of ice leads to an amorphous phase that has a high intrinsic density, $\rho_i = 1.1$ g/cm^3.[36,39,40]

In this work, we combined vacuum microbalance and optical interference techniques to determine directly the density and index of refraction of vapor-deposited ice. Compared to previous work, the current experiments were obtained in better vacuum, and with a well-defined gas flow.

[a]Current address: Cornell University, Department of Applied Physics, Ithaca, New York.
[b]Permanent address: Osservatorio Astrofisico di Catania, Italy.
[c]Author to whom correspondence should be addressed; Electronic mail: raul@virginia.edu

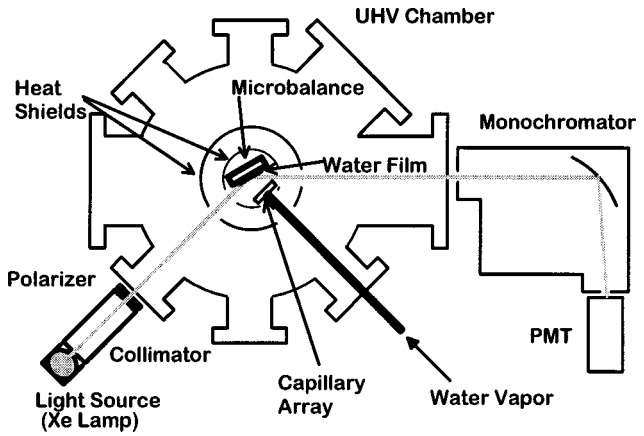

FIG. 1. UHV chamber and schematic of density measurement.

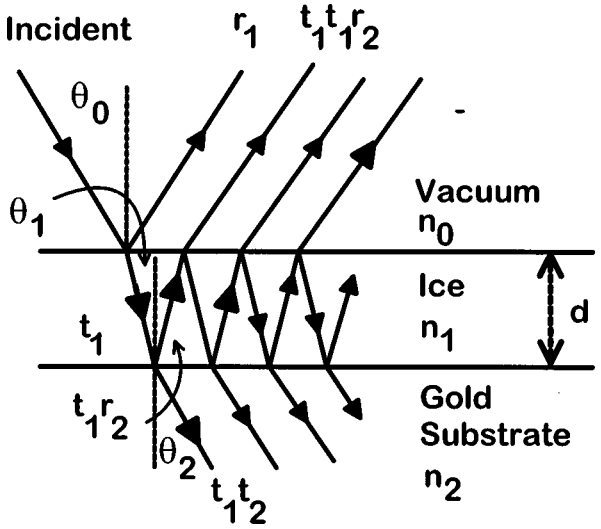

FIG. 2. Reflection from a thin film on a gold substrate.

The density measurements indicate a significant ice porosity that is independent of film thickness. We also determined the density indirectly by using the Lorentz–Lorenz relation. We find that the films are highly transparent (scattering by imperfections is very weak) but they crack and turn white when heated above 150 K.

II. EXPERIMENT

The experiments were performed in a cryopumped ultrahigh vacuum chamber capable of reaching a base pressure of approximately 1×10^{-10} Torr (Fig. 1). The ice films are grown on the optically-flat gold electrode of a quartz crystal resonator[41] used as a microbalance.[5] The crystal holder is attached to a closed-cycle refrigerator and surrounded by two heat shields at about ~30 and 60 K, respectively, which provide additional pumping. The ice films were formed by flowing thoroughly degassed high-purity water vapor through an array of 0.5 mm long, 50 μm diameter capillaries[42] roughly perpendicular to the gold substrate. Effusion from these capillaries should result in a very low fraction of water multimers impacting the surface.[43] Films of thickness between 0.01 and 3 μm were grown at rates in the range 0.6–2 nm/min at substrate temperatures in the 30–140 K temperature interval. The deposition rates are three to four orders of magnitude larger than that of background impurities (mostly H_2 and CO) in the ultrahigh vacuum system, implying high film purity.

The mass of the film is obtained from the change in the resonance frequency of the quartz-crystal microbalance.[5,44] To minimize the effect of the temperature dependence of the resonance frequency, we used a similar resonator placed back to back to the sample crystal, and held at the same temperature but not exposed to the water vapor.[5] A heterodyne circuit measured the difference in frequency. The stability of 0.2 Hz allows detection of a mass change corresponding to 10^{14} water molecules/cm^2, or about 0.1 monolayers.

For the optical interference measurements, collimated white light from a Xe lamp, polarized perpendicular to the plane of incidence, was reflected specularly off the sample at a total scattering angle of $135.4\pm0.9°$. The light was then passed into an optical spectrometer tuned to 435.8 nm with a bandwidth of 2 nm. This wavelength was chosen since it gives quite different indices of refraction of ice and the gold substrate, which leads to a large ratio of maximum to minimum intensity in the interference curves. The measurement of the index of refraction of the gold substrate was made by recording the ratio of the reflected intensities with polarization perpendicular and parallel to the plane of incidence at different incidence angles. From these data, the index of refraction of the substrate (real, imaginary) is $(1.48\pm0.01, -1.78\pm0.01)$, in excellent agreement with published values (1.478, −1.781) for gold.[45]

We measured the reflected intensity during ice growth, while recording the mass deposited per unit area with the microbalance. In addition, we measured nonspecular reflection to monitor surface roughness and scattering in the ice films by turning the sample 10° away from the specular reflection angle. In this position, the background signal (no ice on the substrate) was approximately the dark current level of the photomultiplier detector, showing the absence of any significant scattered light.

For a single, flat surface, the relative magnitude of the reflected (r) and transmitted (t) electric and magnetic vectors for s-polarized light (perpendicular to the plane of incidence) are given by the Fresnel equations,

$$r_{1s}=\frac{n_0\cdot\cos\,\theta_0-n_1\cdot\cos\,\theta_1}{n_0\cdot\cos\,\theta_0+n_1\cdot\cos\,\theta_1},$$

$$t_{1s}=\frac{2\cdot n_0\cdot\cos\,\theta_0}{n_0\cdot\cos\,\theta_0+n_1\cdot\cos\,\theta_1},$$

where n_0 and n_1 are the complex index of refraction of vacuum and the ice film, respectively, and the variables are shown in Fig. 2. The amplitudes of the reflected beams normalized to the incident beam are r_1, r_2, etc., and those of the transmitted beams t_1, t_2, etc. These are the Fresnel coefficients for each of the two interfaces for the incident (no superscript) and reflected (with a $-$superscript) directions. Snell's law relates the angles of incidence with the indices of refraction, $n_1 \sin\theta_1 = n_0 \sin\theta_0$. Also, we must include the

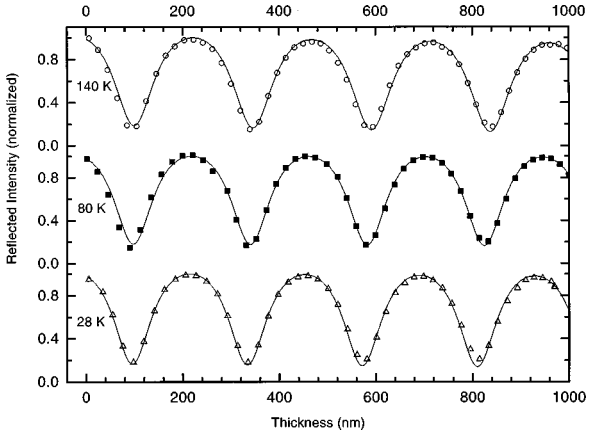

FIG. 3. Examples of interference data and fits for ices grown at different temperatures.

phase change of the light as it passes through the film, given by $\delta_1 = 2\pi n_1 d_1 \cos\theta_1$. The magnitude of the reflected light wave, R, results from summing all reflected rays (there are an infinite number),

$$R = r_1 + t_1 t_1^- r_2 e^{-2i\partial_1} - t_1 t_1^- r_1 r_2^2 e^{-4i\partial_1} + \cdots$$

$$= r_1 + \frac{t_1 t_1^- r_2 e^{-2i\partial_1}}{1 + r_1 r_2 e^{-2i\partial_1}}.$$

Using conservation of energy, $t_1 t_1^- = 1 - r_1^2$, the expression becomes

$$R = \frac{r_1 + r_2 e^{-2i\delta_1}}{1 + r_1 r_2 e^{-2i\delta_1}},$$

from which we obtain $|R|^2$, the observed reflected intensity. We note that the thickness of the film is contained in the exponential expression, and the indices of refraction in the Fresnel coefficients and also in the exponential expression. A more detailed treatment can be found elsewhere.[46]

III. RESULTS

A. Optical constants

Measurements of the density and complex index of refraction were made over a range of growth temperatures, growth rates, and ice film thicknesses. Figure 3 shows examples of interference curves and fits. On first approximation, densities can be determined from the mass deposited between interference maxima and minima. This corresponds to a thickness of $d_m = \lambda/2n_1 \cos\theta_1$, where λ is the wavelength of the light. Since the distance between maxima or between minima remained constant to within 1%–2% during film deposition the density of the films did not change significantly during growth for these 0.1–3 μm films. Also, one can estimate the refractive index from the ratio between the maximum and minimum reflected intensity. It can be noticed in Fig. 3 that the decrease in the amplitude of the oscillations with thickness is very small, indicating that the films are flat and homogeneous with a small loss coefficient and a smooth surface.[46–49]

A more precise determination of film properties results from fitting the complete interference patterns to the equations given above. The results of the fits can be found in Figs. 4 and 5, which show no obvious temperature or growth rate dependence over the range of parameters studied. The value of the density, averaged over all the fits, is 0.82 g/cm^3 with an estimated error of 0.01 g/cm^3. The real part of the index of refraction is 1.29 ± 0.01. This is smaller than the value[50] of 1.316 at 435.8 nm for hexagonal ice ($\rho = 0.92$ g/cm^3 at these temperatures),[1] indicating less dense films. The small scattering coefficients, between 10^{-2} and 10^{-4}, confirmed by nonspecular reflection experiments, may result from Rayleigh scattering from micropores[51] or from surface roughness.

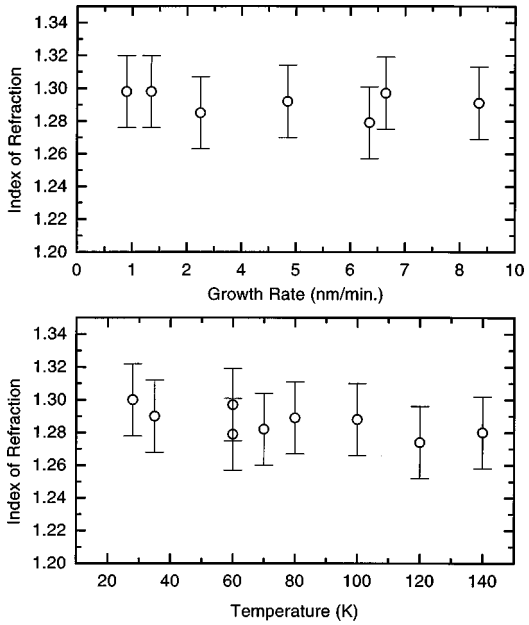

FIG. 4. Index of refraction of ice vs growth temperature and growth rate.

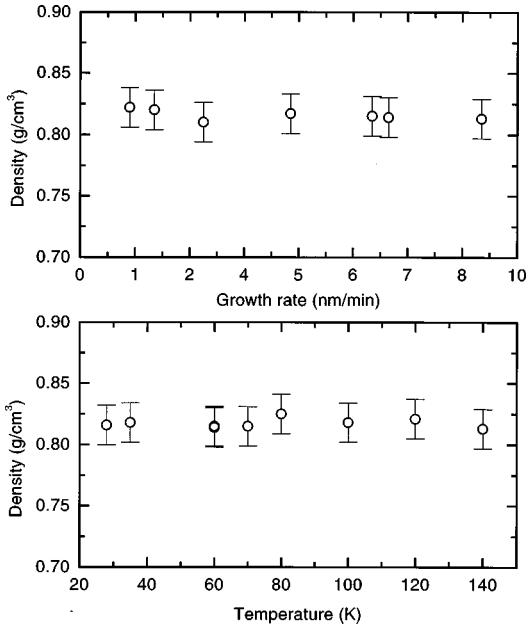

FIG. 5. Density of ice vs growth temperature and growth rate.

B. Density and porosity

The density we measured, 0.82 g/cm^3, agrees within experimental error with that measured by Seiber *et al.* at 82 K, using a very similar technique. We note that at the lowest temperature we obtain much denser films than in some recent reports. The independence of the density on growth rate contrasts with the strong dependence found by Bertand *et al.*,[14] who argue that high condensation rates limit the time for lateral diffusion following adsorption thus producing a lower density film.

From the density, we can estimate the porosity and average pore size. By comparing the average density measured here (which includes pore volume) to the intrinsic density measured by x-ray diffraction[36] (which does not include pore volume), we derive a fractional porosity $p=0.13\pm0.01$ for our ice films. One can also derive the density and porosity from the measured index of refraction n_a using the Lorentz–Lorenz equation[29] which relates p with n_a and the intrinsic index of refraction of bulk ice (regions without pores), n_i,

$$p=1-\frac{\rho_a}{\rho_i}=1-\frac{n_a^2-1}{n_a^2+2}\cdot\frac{n_i^2+2}{n_i^2-1},$$

where ρ_i and ρ_a are the intrinsic and average density values, respectively. Using the index of refraction n_i and density ρ_I given for hexagonal ice near the fusion point yields a density of 0.85 ± 0.03 g/cm^3 and a porosity of 0.10 ± 0.03 when compared with $\rho_I=0.94$ g/cm^3 for amorphous ice. The fact that the values of density measured directly with those derived from the index of refraction are equal within errors implies that deviations from the Lorentz–Lorenz law are small. Such deviations might arise by the slight changes in the optical oscillator strengths that occur among different phases. If we assume that the porosity of the solid is accounted for by interconnected spherical voids, we can derive from these values an average pore radius of 1.5 nm, close to the 2 nm derived by Mayer and Pletzer.[31] This microporous structure is what gives amorphous ice its unusually large ability to trap gases, which is important in astronomical environments.[19–22,52,53]

C. Cracking

In a different experiment, a transparent film grown at a rate of 60 μm/h at 100 K to a thickness of $\sim$150 μm thick turned white when heated to $\geqslant$200 K. The variation of diffuse reflectance as a function of sample temperature (Fig. 6) shows that conversion of transparent ice to a highly scattering form occurs at about 200 K, where the ice transforms to the hexagonal phase. This agrees with results by Ghormley and Hochanadel[35] but, in other reports, the sharp increase of reflectance appears at different temperatures. Seiber *et al.*[37,54] found an irreversible and abrupt increase of reflectance at 145–150 K which they correlated with crystallization of amorphous ice to the cubic phase. Drobishev[10,12] also reported a large and abrupt change in reflectance when warming the ice films but at a higher temperature, 160–162 K, which they correlated to the transformation to the hexagonal phase. We examined the films visually to understand the reason for the increase in reflectivity. At first, films were transparent, then upon warming to about 150 K, a few cracks developed, but the area between the cracks remained transparent. Then, as the film temperature approached 200 K, the different grains began to turn white, one by one, which corresponded to the increase in scattered light seen in Fig. 6. Related to our observations are those of Sivakumar *et al.*.[55] who found that films deposited at 110 K broke up when heated or cooled and those of Wood and Smith[27] who reported that films deposited at 77 K shatter when their thickness exceeds a few microns. This behavior, and the resulting frosted appearance, are possibly related to stresses resulting from changes in the density of the ice, since micropores collapse during annealing.[56,57] It is possible that the variability of the results of different workers for the temperature at which cracks or scattering defects appear is related to the difference in elastic properties between the ice films and the various substrates that have been used. This hypothesis points to a direction for further investigation.

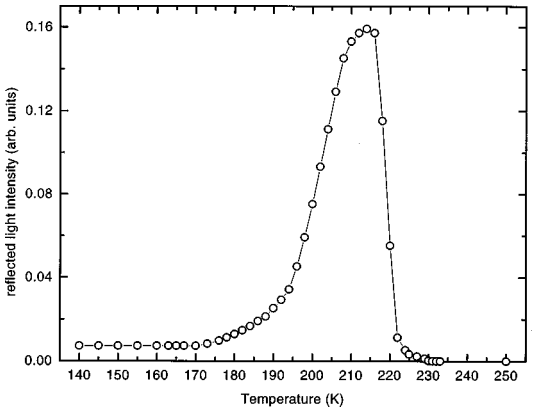

FIG. 6. Nonspecular scattered intensity vs temperature for a $\sim$150 μm thick ice film grown at 100 K.

IV. DISCUSSION

In contrast with previous work, our ice films exhibit good optical properties and relatively high density independent of growth conditions. Much larger porosities than reported here, up to 0.6, have been given in several reports.[20,26,58] Three differences in experimental conditions could be identified with past work; difference in the substrate, direction of water flow, and vacuum conditions. Regarding the effect of the substrate, Rice *et al.*[59] report that the high-density form of amorphous ice, formed on single crystal Cu could not be deposited onto polycrystalline metal or sapphire substrates. Recent studies[6,7] found that the sublimation rates of thin water ice films depend on the substrate where they were grown but that the crystallization kinetics are independent of substrate. This suggests that the morphology rather than the ratio of amorphous to crystalline content depends on the substrate. On the other hand, Brown *et al.*[14,15] obtain similar values for the index of refraction and porosity for films grown on sapphire and in Ru(001).

Differences in the direction of vapor flow may be relevant. In our experiments, water vapor is directed through the surface from an array of capillary tubes of high aspect ratio, which form narrow molecular beams. In contrast,

George and collaborators[13–15,28] dose their samples by having an ambient pressure of water vapor in their vacuum chamber (10^{-6}–5×10^{-5} Torr). Under similar growth conditions Drobyshev[12] obtained a temperature dependence of the index of refraction at 14 μm that implies an ice density that decreases with decreasing temperature. In contrast, Givan *et al.*,[38] who use monodirectional deposition from a single narrow nozzle, find that ice condensed onto CsI at 5 K does not have a measurable porosity. We propose that the direction of the gas flow has an important effect in film density and morphology. Condensing by exposing the substrate to an ambient pressure implies all angles of incidence of the molecules on the surface. At the pressures normally used in vacuum deposition the mean free path of molecules exceeds the dimensions of the vacuum chamber. This means that intermolecular collisions are insufficient to randomize the different water fluxes coming from walls having different properties like temperature, roughness, etc. It is likely that omnidirectional but anisotropic flow will favor the formation of pores when randomly occurring surface structures[60,61] shadow molecules coming from oblique angles.[62,63]

V. CONCLUSIONS

Ice films of high optical quality and relatively high density have been grown by vapor deposition at low temperatures. The density of vapor deposited amorphous water ice was measured directly to be 0.82 ± 0.01 g/cm^3, roughly independent of growth temperature and growth rate. The index of refraction at 435.8 nm is 1.29 ± 0.01, and scattering coefficients between 1×10^{-2} and 1×10^{-4}. The porosity of the ice samples, 0.10 ± 0.03, obtained by two independent methods, is consistent with the gas-trapping ability of amorphous ice. The homogenous, transparent, and flat films that we observe differ from some previous measurements of amorphous ice.

The fact that the ice films obtained at the lowest temperatures are more compact than those reported previously suggests the possible influence of experimental conditions that have not been considered relevant in the past. A significant factor may be that our films where produced from a collimated flow of gas incident roughly normal to the surface of the film which contrasts with omnidirectional flow in previous studies.

We have observed cracking of the films upon warming to 180–200 K which we identify as the source of the previously unexplained increase in diffuse reflectivity. The cracks develop due to contraction of the ice upon annealing and are likely influenced by the degree of mismatch of the elastic properties of the ice films and the substrate. The cracks may lead to the abrupt gas release that was recently reported to occur while heating ice overlayers that had been deposited on top of more volatile CCl_4 films.[64]

ACKNOWLEDGMENTS

This work was supported by NASA-Geophysics program and by a NASA Graduate Research Fellowship to M.S.W. One of us (R.A.B.) acknowledges useful discussions with Dr. B. E. Wood.

[1] P. V. Hobbs, *Ice Physics* (Clarendon P, Oxford, 1974).
[2] *Water: A Comprehensive Treatise*, edited by F. Franks (Plenum, New York, 1982), Vol. 7.
[3] *Ices in the Solar System*, edited by J. Klinger, D. Benest, A. Dollfus, and R. Smoluchowski (Reidel, Dordrecht, 1985).
[4] P. Echlin, *Low-Temperature Microscopy and Analysis* (Plenum, New York, 1992).
[5] N. J. Sack and R. A. Baragiola, Phys. Rev. B **48**, 9973 (1993).
[6] R. S. Smith, C. Huang, E. K. L. Wong, and B. D. Kay, Surf. Sci. **367**, L13 (1996).
[7] P. Löfgren, P. Ahlström, D. V. Chakarov, J. Lausmaa, and B. Kasemo, Surf. Sci. **367**, L19 (1996).
[8] A. Kouchi, J. M. Greenberg, T. Yamamoto, and T. Mukai, Astron. J. **388**, L73 (1992).
[9] O. Andersson and H. Suga, Solid State Commun. **91**, 985 (1994).
[10] C. E. Bryson, V. Cazcarra, and L. L. Levenson, J. Vac. Sci. Technol. **11**, 411 (1974).
[11] A. S. Drobyshev, N. V. Atapina, D. N. Garipogly, S. L. Maksimov, and E. A. Samyshkin, Low Temp. Phys. **19**, 404 (1993).
[12] A. S. Drobyshev, Low Temp. Phys. **22**, 123 (1996).
[13] D. R. Haynes, N. J. Tro, and S. M. George, J. Phys. Chem. **96**, 8502 (1992).
[14] B. S. Berland, D. E. Brown, M. A. Tolbert, and S. M. George, JGR Lett. **22**, 3493 (1995).
[15] D. E. Brown, S. M. George, C. Huang, E. K. L. Wong, K. Rider, R. S. Smith, and B. Kay, J. Phys. Chem. **100**, 4988 (1996).
[16] J. A. Ghormley, J. Chem. Phys. **46**, 1321 (1967).
[17] A. W. Adamson, L. M. Dormant, and M. Orem, J. Colloid Interface Sci. **25**, 206 (1967).
[18] J. Ocampo and J. Klinger, J. Colloid Interface Sci. **86**, 377 (1982).
[19] E. Mayer and R. Pletzer, Nature (London) **319**, 298 (1986).
[20] A. Bar-Nun, J. Dror, E. Kochavi, and D. Laufer, Phys. Rev. B **35**, 2427 (1987).
[21] D. Laufer, E. Kochavi, and A. Bar-Nun, Phys. Rev. B **36**, 9219 (1987).
[22] A. Bar-Nun, I. Kleinfeld, and E. Kochavi, Phys. Rev. **38,** 7749 (1988).
[23] J. P. Devlin, J. Phys. Chem. **96**, 6185 (1992).
[24] B. Schmitt, S. R. J. A. Grim, J. M. Greenberg, and J. Klinger, in *Physics and Chemistry of Ices*, edited by N. Maeno and T. Hondoh (Hokkaido University, Sapporo, 1992).
[25] J. Hessinger and R. O. Pohl, J. Non-Cryst. Solids **208**, 151 (1996).
[26] J. Kruger and W. J. Ambs, J. Opt. Soc. Am. **40**, 1195 (1959); **40**, 1415 (1959).
[27] B. E. Wood and A. M. Smith, in *Thermophysics and Thermal Control*, Vol. 65 in *Progress in Astronautics and Aeronautics* (American Institute of Aeronautics and Astronautics, New York, 1978), p. 22.
[28] B. S. Berland, D. R. Haynes, K. L. Foster, M. A. Tolbert, S. M. George, and O. B. Toon, J. Phys. Chem. **98**, 4358 (1994).
[29] M. Born and E. Wolf. *Principles of Optics* (Pergamon, Oxford, 1975).
[30] F. Spinella, G. A. Baratta, G. Strazzulla, and L. Torrisi, Radiat. Eff. Defects Solids **115**, 307 (1991).
[31] E. Mayer and R. Pletzer, J. Chem. Phys. **80**, 2939 (1984).
[32] R. J. Speedy, J. Phys. Chem. **96**, 2322 (1992).
[33] P. Jenniskens and D. Blake, Science **265**, 754 (1994).
[34] P. Jenniskens, D. F. Blake, M. A. Wilson, and A. Pohorille, Astron. J. **473**, 1104 (1996).
[35] J. A. Ghormley and C. J. Hochanadel, Science **171**, 62 (1971).
[36] A. H. Narten, C. G. Venkatesh, and S. A. Rice, J. Chem. Phys. **64**, 1106 (1976).
[37] B. A. Seiber, B. E. Wood, A. M. Smith, and P. R. Müller, Science **170**, 652 (1970).
[38] A. Givan, A. Loewenschuss, and C. J. Nielsen, Vib. Spectrosc. **12**, 1 (1996); J. Phys. Chem. B **101**, 8696 (1997).
[39] H. G. Heide and E. Zeitler, Ultramicroscopy **16**, 151 (1985).
[40] P. Jenniskens, D. F. Blake, M. A. Wilson, and A. Pohorille, Astron. J. **455**, 389 (1995).
[41] McCoy Electronics (Mt. Holy Springs, PA).
[42] Galileo (Sturbridge, MA) C26S10M50 capillary array.
[43] T. A. Milne, J. E. Beachey, and F. T. Greene, J. Chem. Phys. **57**, 2221 (1972).
[44] C. Lu and O. Lewis, J. Appl. Phys. **56**, 608 (1984).
[45] *CRC Handbook of Chemistry and Physics* (Chemical Rubber, Florida, 1985).

[46] O. S. Heavens, *Optical Properties of Thin Solid Films* (Dover, New York, 1991).
[47] H. K. Pulker, Appl. Opt. **18**, 1969 (1979).
[48] A. M. Goodman, Appl. Opt. **17**, 2779 (1978).
[49] R. P. Kusy, J. M. Stuart, J. Q. Whitney, and C. R. Saunders, J. Am. Ceram. Soc. **76**, 299 (1993).
[50] S. G. Warren, Appl. Opt. **25**, 2650 (1986).
[51] B. Crosignani, P. D. Porto, and M. Bertolotti, *Statistical Properties of Scattered Light* (Academic, New York, 1975).
[52] A. Kouchi and T. Yamamoto, Prog. Cryst. Growth Charact. Mater. **30**, 83 (1995).
[53] R. A. Vidal, D. Bahr, R. A. Baragiola, and M. Peters, Science **276**, 1839 (1997).
[54] B. E. Wood, A. M. Smith, J. A. Roux, and B. A. Seiber, AIAA J. **9**, 1836 (1971).
[55] T. C. Sivakumar, S. A. Rice, and M. G. Sceats, J. Chem. Phys. **69**, 3468 (1978).
[56] B. Rowland and J. P. Devlin, J. Chem. Phys. **94**, 812 (1991); B. Rowland, M. Fisher, and J. P. Devlin, *ibid.* **95**, 1378 (1991).
[57] B. Rowland, M. Fisher, and J. P. Devlin, J. Chem. Phys. **95**, 1378 (1991).
[58] J. Hessinger, B. E. White, and R. O. Pohl, Planet. Space Sci. **44**, 937 (1996).
[59] S. A. Rice, W. G. Madden, R. McGraw, M. G. Sceats, and M. S. Bergren, J. Glaciol. **85**, 509 (1978).
[60] V. Buch, J. Chem. Phys. **96**, 3814 (1992).
[61] U. Essmann and A. Geiger, J. Chem. Phys. **103**, 4678 (1995).
[62] A. L. Barabasi and H. E. Stanley, *Fractal Concepts in Surface Growth* (Cambridge University Press, Cambridge, 1995).
[63] M. A. Wilson, A. Pohorille, P. Jenniskens, and D. F. Blake, in *Origin of Life and Evolution of the Biosphere 25, 3-19* (Kluwer Academic, Amsterdam, 1995).
[64] R. S. Smith, C. Huang, F. K. L. Wong, and B. D. Kay, Phys. Rev. Lett. **79**, 909 (1997).